On Stabilization of Multi-Layer Hele-Shaw and Porous Media Flows in the Presence of Gravity

Prabir Daripa*
Department of Mathematics
Texas A&M University
College Station, TX-77843, USA

June 30, 2012

Abstract

Stabilization of multi-layer Hele-Shaw flows is studied here by including the influence of Rayleigh-Taylor instability in our earlier work [Daripa P, 2008, J. Stat. Mech. Article P12005, DOI: 10.1088/1742-5468/2008/12/P12005] on stabilization of multi-layer Saffman-Taylor instability. Furthermore, this article goes beyond our previous work with few extensions, improvements, new interpretations, and clarifications on the use of some terminologies. Results of two complete studies have been presented: the first investigates the effect of individually unstable interfaces on the overall stability of the flow, and the second studies the cumulative effect of unstable interfaces as well as unstable internal viscous layers. In each case, modal and absolute upper bounds on the growth rate are reported. Next, these bounds are used to investigate (i) stabilization of long waves on various interfaces; (ii) stabilization of all waves on all interfaces in comparison to pure Taylor instability; (iii) stabilization of disturbances on interior interfaces instead of exterior interfaces. In the first study, notions of partial and total stabilization with respect to the pure Taylor growth rate are introduced. Then necessary and sufficient conditions for partial and total stabilizations are found. Proof of stabilization of long waves on one of the two external interfaces in multi-layer flows is also proved. In the second study, an absolute upper bound is obtained in the presence of stabilizing density stratification across each internal interface even though all interfaces and layers have unstable viscous profiles. Exact results on the upper bounds, and necessary and sufficient conditions for control of instabilities driven by stable/unstable density stratification, unstable viscous layers and unstable interfaces are new and may be relevant to explain observed phenomena in many complex flows generating these kinds of viscous profiles and density stratification as they evolve. The present work builds upon and goes much further in details and new results than our previous work. The gravity effect included here brings with it restrictions which have not been addressed before in this multi-layer context.

Keywords: Multi-layer Hele-Shaw flows, Linear Stability, Upper bound.

*e-mail: prabir.daripa@math.tamu.edu

1 Introduction

It is well known that fluid flow through porous media is a very important topic of fundamental and applied research. It occurs in nature as well as in a wide variety of applications such as in oil recovery, drainage of fluids through soil and subsurface formations, just to name a few. Advances in understanding of porous media flow through research can have immediate positive impact worldwide. The complexity of fluid flow and level of modeling difficulty depend on several factors such as heterogeneity of media properties, wettability properties of the medium, number of fluid phases flowing, nonlinearity in capillary pressure dependence on concentrations of various phases and chemicals, initial data of various phases, chemicals etc., dynamic development of coherent structures such as fingering at various scales, and number of displacing fluids in cases where goal is to displace a particular fluid such as oil in oil recovery. Collective effect of all of these factors on fluid flow may not always be desirable and when that is the case, it becomes necessary to control some of the factors that may lead to desirable outcome. An understanding of the effect of each of these factors in isolation may be helpful in this regard. With this goal in mind, the purpose in this paper is to estimate the collective effect of multiple displacing fluids on the Taylor stability of the interfaces that sweep a displaced fluid in homogeneous porous media. This study has relevance to chemical enhanced oil recovery (see Daripa & Ding [6]). It has been argued in Daripa [5] that fluid flow in homogeneous porous media is analogous to Hele-Shaw flow so long as the effect of rarefaction waves of saturation is negligible. Because of this analogy, the study below refers to Hele-Shaw flow only for brevity.

The displacement of a more viscous fluid by a less viscous one is known to be potentially unstable in a Hele-Shaw cell (see [11]). This is also known as the Saffman-Taylor instability [18]. Similarly, stratified flows are gravitationally unstable if the gravitational acceleration acts in the direction of negative density gradient. This is known as the Rayleigh-Taylor instability. Therefore, if a fluid displaces another fluid of different viscosity and different density in the presence of gravity, then the interface will be influenced by a combination of Saffman-Taylor and Rayleigh-Taylor instabilities. Depending on the viscosity and density jumps across an interface, these two instabilities can either reinforce or attenuate each other. Exact linearized growth rates of small amplitude interfacial disturbances for such single-interface flows are well known in the literature and well-documented in standard textbooks on hydrodynamic stability theory, e.g. Drazin & Reid [9]. For our purposes below, it is worth citing here some exact results for rectilinear flows. If (μ_r, ρ_r) are the (viscosity, density) of the displaced fluid, $(\mu_l < \mu_r, \rho_l)$ are the (viscosity, density) of the displacing fluid, U is the constant velocity of the rectilinear flow, gravity g is in the direction of U, and the interfacial tension at the interface is T, then the **pure Taylor growth rate** σ_t of the interfacial disturbance having wave-number k is given by

$$\sigma_t(k) = \frac{k(U(\mu_r - \mu_l) - g(\rho_r - \rho_l)) - k^3 T}{\mu_r + \mu_l}, \tag{1}$$

from which it follows that growth rate of any unstable wave can not exceed σ_t^u:

$$\sigma_t \leq \sigma_t^u = \frac{2T}{(\mu_r + \mu_l)} \left(\frac{U(\mu_r - \mu_l) - g(\rho_r - \rho_l)}{3T} \right)^{3/2}. \tag{2}$$

The pure Taylor growth rate has been used to refer to individual growth rate of disturbances on a single interface due to the combined effect of Saffman-Taylor and Rayleigh-Taylor instabilities. These formulas allow reliable prediction of the effect of interfacial tension and fluid properties across an interface on the growth of the interfacial disturbances. They also help in the selection of correct fluid and interfacial properties a priori in order to control growth rates of interfacial disturbances.

Below, "total stabilization" means all interfaces in multi-layer flows are less unstable in comparison to σ_t^u based on extreme layer fluids, total referring to "all interfaces" and "stabilization" referring to "being less unstable". Similarly "partial stabilization" means at least one interface is less unstable in comparison to σ_t^u. In general, conditions under which partial and total stabilization can be achieved are non-trivial because of the complicated role of interfacial tensions of all interfaces on the collective stability of the system. In [4], this has been addressed in the absence of gravity. In this paper, we study this problem by including gravity and show, in addition to many other properties, how gravity alters the conditions for stabilization. We also classify interfaces in multi-layer flows into two groups as it helps discussing the physical implications of our results. These two groups are: external versus internal interfaces. An external interface has on its one side a fluid layer of infinite extent and an internal interface has on its each side a fluid layer of finite extent which in turn is separated from other fluid layers of either finite or infinite extent. Thus, a 3-layer flow has no internal but two external interfaces, a 4-layer has one internal and two external interfaces and so on. As we will see below, internal and external interfaces are different stability-wise.

For multi-interface flows, there is no mathematical formula analogous to the above two formulas (1) and (2). In the absence of such a theory, it is tempting to use the above two single-interface results locally around each interface thereby ignoring the effects of other interfaces. Such a theory could be misleading and a better alternative is desirable. Recently, Daripa [4] presented such a theory that gives upper bounds on the disturbance growth rates in multi-layer flows but in the absence of gravity. In this paper, we extend our previous work (see [4]) in several respects some of which are *(i) inclusion of the influence of gravity when the density in each layer is constant; (ii) introduction of the notions of partial and total stabilization with respect to the pure Taylor growth rate* σ_t^u*; (iii) necessary and sufficient conditions for partial and total stabilization; and (iv) formulas delineating the distinction between internal and external interfaces from the viewpoint of stability; (v) proof of stabilization of long waves on one of the two external interfaces in multi-layer flows; and (vi) upper bound results for multi-layer flows in the presence of stable and unstable density stratification.* Exact results on the upper bounds, and necessary and sufficient conditions for control of instabilities driven by stable/unstable density stratification and unstable viscous layers and interfaces are new. These results may be relevant for explanation of some observed phenomena in many complex flows involving such viscous and density profiles. The results derived in this paper now make it possible to assess the cumulative effects of all interfacial tensions and viscosity and density jumps across all interfaces on the overall stability of the multi-layer system. The formulas and principles laid out can guide to the selection of fluid properties and interfacial tensions in order to achieve a desired level of stabilization.

The paper is laid out as follows. In section 2, relevant fluid flow equations involving density stratification, unstable viscosity profiles, and unstable viscous jumps at interfaces are presented. Then the eigenvalue problem arising from the stability analysis of these fluid flow equations is presented. In sections 3, 4, and 5, constant viscosity layer cases in the presence of density stratification are treated respectively for 3, 4 and general multi-layer cases. The 3-layer case is the fundamental building block and hence it has been treated first. The internal interface which appears first in the 4-layer case behaves differently from external interfaces as discussed in section 4. Therefore this 4-layer case is treated separately and in detail before generalizing to the case of arbitrary number of layers in section 5. In section 6, we directly treat the case of an arbitrary number of layers in the presence of stable and unstable density stratification when interfaces and internal layers have unstable viscosity profiles. With stable density stratification for internal interfaces, upper bound results in strict inequality form are presented for the general case. Finally we conclude and provide a summary of this work in section 7.

2 Background

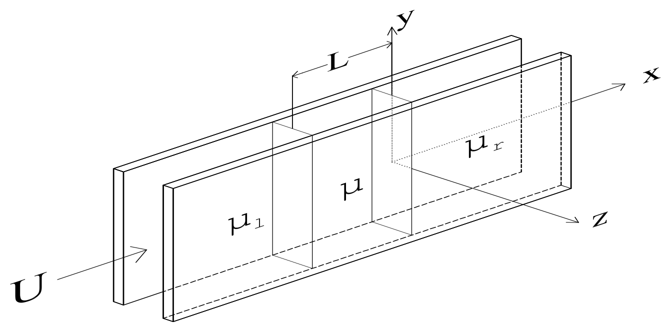

Figure 1: Three-layer fluid flow in a Hele-Shaw cell.

The three-layer case as shown in Fig. 1 is the fundamental building block of the multi-layer case and hence we discuss this case first briefly. Since this paper extends the work of Daripa [4], some degree of overlap is not only unavoidable but also necessary as it enables us to present our work in a more reader-friendly manner without losing any continuity and clarity. The physical set-up and mathematical formulation of the basic flow differs from the one discussed in Daripa [4] only in the effect of gravity which is included in the present model. We briefly describe the present set-up: the physical set-up consists of two-dimensional fluid flows in a three-layer Hele-Shaw cell. The domain Ω of interest is then $\Omega := (x, y) = \mathbb{R}^2$ (with a periodic extension of the set-up in the $y-$direction). The fluid upstream (i.e., as $x \to -\infty$) has a velocity $\mathbf{u} = (U, 0)$. The fluid in the left layer with constant viscosity μ_l extends up to $x = -\infty$, the fluid in the right layer with constant viscosity μ_r extends up to $x = \infty$, and the fluid in-between middle-layer of length L has a smooth viscous profile $\mu(x)$ with $\mu_l < \mu(x) < \mu_r$. Thus ST-instability is present at each of the interfaces. The density in three layers from left to right are respectively ρ_l, ρ_1, and ρ_r with gravity g acting in the direction of flow, i.e. along positive x-axis. The density is constant in each layer with the possibility of density jump at each of the interfaces. Thus each layer is RT-stable (RT stands for Raleigh-Taylor) but an interface can be RT-unstable if density at that interface decreases in the direction of gravity.

The underlying equations of this problem are then given by

$$\nabla\cdot\mathbf{u} = 0, \quad \nabla\, p = -\mu\, \mathbf{u} + \rho\, g\, \mathbf{e}_1, \quad \frac{\partial \mu}{\partial t} + \mathbf{u}\cdot\nabla\mu = 0, \tag{3}$$

where $\nabla = \left(\frac{\partial}{\partial x}, \frac{\partial}{\partial y}\right)$ and $\mathbf{e}_1$ is the unit vector in the $x-$direction. The first equation $(3)_1$ is the continuity equation for incompressible flow, the second equation $(3)_2$ is the Darcy's law ([3]), and the third equation $(3)_3$ is the advection equation for viscosity ([7],[10]). This equation for viscosity arises from the continuity equation of species such as polymer in water which is simply being advected, and viscosity of this poly-solution (polymer in water) is an invertible function of polymer concentration. For further details, we direct the readers to [4] and [7].

The above system admits a simple basic solution: the whole fluid set-up moves with speed U in the x direction and the two interfaces, namely the one separating the left layer from the middle-layer and the other separating the right layer from the middle-layer, are planar (i.e. parallel to the $y-z$-plane). The pressure corresponding to this basic solution is obtained by integrating $(3)_2$. In a frame moving with velocity $(U, 0)$, the above system is stationary along with two planar interfaces separating these three fluid layers. Here and below, with slight abuse of notation, the same variable x is used in the moving reference frame. Linear stability analysis of the basic solution $(u = 0, v = 0, p_0(x), \mu(x))$ in the moving frame leads to the following eigenvalue problem. The eigenfunction $f(x)$ is proportional to the x-directional velocity perturbation and eigenvalue σ is the growth rate of the disturbance with wavenumber k. We refer to [4] for more details on this.

$$\mu\left(f_{xx} - k^2 f\right) + \mu_x f_x + \frac{k^2 U}{\sigma}\mu_x f = 0, \quad x \neq -L, 0. \tag{4}$$

$$f_{xx} - k^2 f = 0, \quad x < -L, \ x > 0, \tag{5}$$

with far-field behavior given by

$$f(x) = f(-L)\exp(k(x+L)), \quad \text{for} \quad x < -L, \quad f(x) = f(0)\exp(-kx), \quad \text{for} \quad x > 0. \tag{6}$$

Following the procedure sketched in Daripa [4], interfacial conditions in the presence of gravity and density stratification are

$$\left.\begin{aligned} -(\mu^- f_x^- f)(0) &= \mu_r\, k\, f^2(0) - \tfrac{E_0}{\sigma}\, f^2(0), \\ (\mu^+ f_x^+ f)(-L) &= \mu_l\, k\, f^2(-L) - \tfrac{E_1}{\sigma}\, f^2(-L), \end{aligned}\right\} \tag{7}$$

where

$$E_0 = k^2(U[\mu]_r - g[\rho]_r) - T_0\, k^4, \quad E_1 = k^2(U[\mu]_l - g[\rho]_l) - T_1\, k^4. \tag{8}$$

Above $[\mu]_r = (\mu_r - \mu^-(0))$, and $[\mu]_l = (\mu^+(-L) - \mu_l)$. Similarly, for $[\rho]_r$ and $[\rho]_l$. The mathematical problem for this three-layer case is defined by the field equation (4), far-field boundary conditions (6) and two interfacial conditions (7). Note that boundary conditions (7) depend on the gravity through the definition of E_0 and E_1 in (8).

3 Constant viscosity fluid layers: Three-layer case

Both, Saffman-Taylor and Rayleigh-Taylor, instabilities now play a role as opposed to our earlier study [4] of Saffman-Taylor instability in the multi-layer case. These two instabilities can act in a way to either reinforce or weaken the overall instability of the system depending on the situation. Viscosity driven layer-instability and interfacial-instability appear in our model through the field equation (4) and the boundary conditions (7) respectively. Their roles for the instability of multi-layer flows have been well explored in several of our recent papers (see[4], [5], [6]). The current model also includes the gravity driven instability through the boundary conditions (7) which were otherwise absent in all of our studies so far. The three-layer case here with constant viscosity and constant density of all layers retain these instabilities only at the interfaces, thereby making it possible to estimate their relative effects on the growth rate as shown below. With constant viscosity μ_1 ($\mu_l < \mu_1 < \mu_r$) of the intermediate layer and using weak formulation of the above underlying equations, one obtains the following Rayleigh-quotient type formula for the growth rate as in Daripa [4].

$$\sigma(k) = \frac{E_0\, f^2(0) + E_1\, f^2(-L)}{\mu_r\, k\, f^2(0) + \mu_l\, k\, f^2(-L) + \mu_1 \int_{-L}^{0} (k^2\, f^2 + f_x^2)\, dx}. \tag{9}$$

All the terms in the denominator above are positive. In this subsection, an estimate of the upper bound will be obtained by neglecting the positive values of integrals in (9) and by making use of the following relation from [8] which holds for arbitrary n under the condition $A_i > 0, B_i > 0, X_i > 0,$ for $i = 1, ..n$,

$$\frac{\sum_i^n (A_i X_i)}{\sum_i^n (B_i X_i)} \le \max_i \left\{ \frac{A_i}{B_i} \right\}. \tag{10}$$

We consider following two non-trivial cases.

Case 1. $U\, [\mu]_l - g\, [\rho]_l > 0$ and $U\, [\mu]_r - g\, [\rho]_r > 0$.

This condition means that both the interfaces are individually unstable. We obtain the following estimates for the growth rates of waves grouped in the following four classes.

$$\text{(i)} \qquad k^2 > \max\left\{ \frac{U\, [\mu]_l - g\, [\rho]_l}{T_1}, \frac{U\, [\mu]_r - g\, [\rho]_r}{T_0} \right\} \Rightarrow E_0 < 0, E_1 < 0 \Rightarrow \sigma < 0. \tag{11}$$

$$\text{(ii)} \qquad \frac{U\, [\mu]_r - g\, [\rho]_r}{T_0} < k^2 < \frac{U\, [\mu]_l - g\, [\rho]_l}{T_1} \Rightarrow E_0 < 0, E_1 > 0 \Rightarrow \sigma < \frac{E_1}{\mu_l k}. \tag{12}$$

$$\text{(iii)} \qquad \frac{U\, [\mu]_l - g\, [\rho]_l}{T_1} < k^2 < \frac{U\, [\mu]_r - g\, [\rho]_r}{T_0} \Rightarrow E_0 > 0, E_1 < 0 \Rightarrow \sigma < \frac{E_0}{\mu_r k}. \tag{13}$$

$$\text{(iv)} \qquad k^2 < \min\left\{ \frac{U\, [\mu]_l - g\, [\rho]_l}{T_1}, \frac{U\, [\mu]_r - g\, [\rho]_r}{T_0} \right\} \Rightarrow E_0 > 0, E_1 > 0. \tag{14}$$

Therefore, we obtain for nontrivial disturbance in the range (14), (15)

$$\begin{aligned} \sigma(k) &< \frac{E_0 f^2(0) + E_1 f^2(-L)}{\mu_r k f^2(0) + \mu_l k f^2(-L)} < \max\left\{ \frac{E_0}{k\mu_r}, \frac{E_1}{k\mu_l} \right\} \\ &= \max\left\{ \left(\frac{(U[\mu]_r - g[\rho]_r)\, k - T_0 k^3}{\mu_r} \right), \left(\frac{(U[\mu]_l - g[\rho]_l)k - T_1 k^3}{\mu_l} \right) \right\}. \end{aligned} \tag{16}$$

Since the upper bound (16) is not less than the estimates (12) and (13) for the upper bounds on growth rates for waves outside the range (14), (16) is a modal upper bound for all waves. The absolute upper bound (i.e., the growth rate of any unstable wave can not exceed this bound) is then given by

$$\sigma < \max\left\{ \frac{2T_0}{\mu_r} \left(\frac{U[\mu]_r - g[\rho]_r}{3T_0} \right)^{3/2}, \frac{2T_1}{\mu_l} \left(\frac{U[\mu]_l - g[\rho]_l}{3T_1} \right)^{3/2} \right\}. \tag{17}$$

Case 2. $U\, [\mu]_l - g\, [\rho]_l < 0$ and $U\, [\mu]_r - g\, [\rho]_r > 0$ or $U\, [\mu]_l - g\, [\rho]_l > 0$ and $U\, [\mu]_r - g\, [\rho]_r < 0$.

Since only one of the two interfaces remains effectively unstable in the presence of gravity, it easily follows from similar analysis as given above that

$$\left.\begin{array}{ll} \sigma < \frac{2T_0}{\mu_r}\left(\frac{U[\mu]_r - g[\rho]_r}{3T_0}\right)^{3/2}, & \text{if } U\,[\mu]_l - g\,[\rho]_l < 0 \text{ and } U\,[\mu]_r - g\,[\rho]_r > 0. \\ \sigma < \frac{2T_1}{\mu_l}\left(\frac{U[\mu]_l - g[\rho]_l}{3T_1}\right)^{3/2}, & \text{if } U\,[\mu]_l - g\,[\rho]_l > 0 \text{ and } U\,[\mu]_r - g\,[\rho]_r < 0. \end{array}\right\} \tag{18}$$

Note that this case is actually covered by (17) as one of the terms in (17) is negative. Therefore, the distinction between the two cases given above will not be made below and the strict inequality (17) or its improved equivalent version will be used for all cases involving at least one unstable interface. This covers the above two cases: Case 1 and Case 2.

Later, we give an estimate for the integral in the denominator of (9) which was neglected in deriving the above formulas (16) and (17). This estimate of the integral will then be used to obtain an improved estimate of the upper bound which, as we will see, is an improvement over (16) and (17) in some sense. Still the bound given above is useful as we will see when we compare these two upper bounds.

3.1 A lemma

The following lemma proof of which can be found in [4] will be used below to obtain a stronger result on the upper bound than the one given above (i.e., the inequality (17)).

Lemma 1. *Consider the function f and the integral I such that*

$$f_{xx}(x) - k^2 f(x) = 0, \quad \forall\, x \in (-L, 0), \quad I = \int_{-L}^{0} (k^2 f^2 + f_x^2)dx. \tag{19}$$

Then we have the following inequality

$$I \geq \max\left\{k\, \tanh(kL) f^2(-L),\; k\, \tanh(kL) f^2(0)\right\} \geq k\, \tanh(kL)(\lambda_1\, f^2(-L) + \lambda_2\, f^2(0)), \tag{20}$$

where $\lambda_i \geq 0$, and $\lambda_1 + \lambda_2 \leq 1$. For non-trivial disturbance f, the second inequality above should be taken as a strict inequality when both the parameters λ_1 and λ_2 are simultaneously zero.

The lemma given in [4] has been modified above by the last sentence. For purposes below, it is useful to recall the following notations from Daripa [4].

3.2 Some notations

- $\lambda_{i,j}$: This notation is a generalization of the notation λ_1 and λ_2 used in the lemma above. This is required for multi-layer flows as we will see in later sections. First subscript 'i' on $\lambda_{i,j}$ can be either 1 or 2 in the spirit of the lemma (see (20)). As we will see below, an inequality of the type (20) will appear for each internal layer for multi-layer flows. The second index 'j' on $\lambda_{i,j}$ refers to the specific internal layer number 'j' in multi-layer flows. Below, we do not use this second index when there is only one internal layer, i.e., in the three-layer case because there is no source of confusion in not using this second index in this case. In general, however, for more than one-internal layer flows we will use $\lambda_{1,j}$ and $\lambda_{2,j}$ instead of λ_1 and λ_2 when using the above lemma.

- $\sigma_n(k)$: This notation stands for **exact** value of the growth rate $\sigma_n(k)$ of a mode with wavenumber k in $(n+2)$-layer Hele-Shaw flows which has n-internal layers ($n = 1, 2, N$ are of interest below).

- $\sigma_n^m(k;\lambda_{i,j})$: This notation stands for **modal upper bound** on $\sigma_n(k)$ which depends on parameters $\lambda_{i,j}$. In other words, $\sigma_n(k) \le \sigma_n^m(k;\lambda_{i,j})$ for all allowable values of $\lambda_{i,j}$ according to Lemma 1. Exact number of parameters it will depend on will be exactly $2n$ and it will be explicit in the expression for $\sigma_n^m(k;\lambda_{i,j})$.

- $\sigma_n^m(k)$: This stands for **modal upper bound independent of parameters** $\lambda_{i,j}$. Physically, this is of interest. Thus it is defined as

$$\min_{\lambda_{1,j}+\lambda_{2,j}\le 1} \sigma_n^m(k;\lambda_{i,j}) \le \sigma_n^m(k).$$

  This minimum is to be taken over all layers, i.e., $\lambda_{1,j}+\lambda_{2,j} \le 1,\ \forall\ 1 \le j \le n$.

- $\sigma_n^u(\lambda_{i,j})$: This is the **absolute upper bound** over all wavenumbers for any specific choice of parameters within the constraint of the Lemma.

- σ_n^u: This is the **absolute upper bound** over all wavenumbers and over all allowable values of the parameters $\lambda_{i,j}$. Growth rates can not exceed this value regardless of the value of k and parameters $\lambda_{i,j}$. Thus

$$\max_k \sigma_n^m(k) \le \sigma_n^u.$$

Below, when necessary we will use either s or l subscript on σ in addition to n to denote short wave or long wave regimes respectively.

3.3 Improved estimates of modal and absolute upper bounds

The effective modal growth rates $Q_l(k,\lambda_1)$ and $Q_r(k,\lambda_2)$ of disturbances on the trailing (left) and leading (right) interfaces respectively are given by (see Daripa [4]).

$$\left.\begin{aligned} Q_l(k,\lambda_1) &= k(U[\mu]_l - g[\rho]_l - T_1k^2)/(\mu_l + \lambda_1\mu_1\tanh(kL)),\\ Q_r(k,\lambda_2) &= k(U[\mu]_r - g[\rho]_r - T_0k^2)/(\mu_r + \lambda_2\mu_1\tanh(kL)),\end{aligned}\right\} \tag{21}$$

and an improved estimate for the upper bound in terms of these is given by

$$\sigma_1(k) \le \max\{Q_l(k,\lambda_1), Q_r(k,\lambda_2)\} = \sigma_1^m(k;\lambda_1,\lambda_2).$$

For best possible estimate of the upper bound within the limitation of the Lemma, we need to use values of (λ_1,λ_2) for which the estimate (22) is minimum over all admissible values of λ_1 and λ_2. Therefore, using the Lemma, it is clear from the expression (22) that desired estimate $\sigma_1^m(k)$ of the modal upper bound over all allowable values of λ_1 and λ_2 is given by

$$\begin{aligned}\sigma_1(k) \le \min\Bigg(&\max\left\{\frac{k(U[\mu]_l - g[\rho]_l) - T_1k^3}{\mu_l + \mu_1\tanh(kL)},\ \frac{k(U[\mu]_r - g[\rho]_r) - T_0k^3}{\mu_r}\right\},\\ &\max\left\{\frac{k(U[\mu]_l - g[\rho]_l) - T_1k^3}{\mu_l}, \frac{k(U[\mu]_r - g[\rho]_r) - T_0k^3}{\mu_r + \mu_1\tanh(kL)}\right\}\Bigg)\\ = \sigma_1^m(k).\end{aligned} \tag{22}$$

If $(U[\mu]_r - g[\rho]_r) \le 0$, then obviously the ratio involving this in the above inequality drops out. Similarly if $U[\mu]_l - g[\rho]_l \le 0$. When both of these are not true, (i.e. when all interfaces are individually unstable), the functions $Q_l(k, \lambda_1 = 0)$ and $Q_r(k, \lambda_2 = 0)$ take their maximum values $Q_{l,\max}(\lambda_1 = 0)$ and $Q_{r,\max}(\lambda_2 = 0)$ at $k = k_{c1}$ and $k = k_{c0}$ respectively which are given by

$$\left.\begin{array}{ll} k_{c1} = \sqrt{\frac{U[\mu]_l - g[\rho]_l}{3T_1}}, & k_{c0} = \sqrt{\frac{U[\mu]_r - g[\rho]_r}{3T_0}}, \\ Q_{l,\max}(\lambda_1 = 0) = \frac{2T_1}{\mu_l}\left(\frac{U[\mu]_l - g[\rho]_l}{3T_1}\right)^{3/2}, & Q_{r,\max}(\lambda_2 = 0) = \frac{2T_0}{\mu_r}\left(\frac{U[\mu]_r - g[\rho]_r}{3T_0}\right)^{3/2}. \end{array}\right\} \tag{23}$$

The following improved estimate σ_1^u of the absolute upper bound follows from (22) and (23).

$$\begin{aligned} \sigma_1(k) \le \min\Bigg(&\max\left\{Q_{l,\max}(\lambda_1 = 1), \frac{2T_0}{\mu_r}\left(\frac{U[\mu]_r - g[\rho]_r}{3T_0}\right)^{3/2}\right\}, \\ &\max\left\{\frac{2T_1}{\mu_l}\left(\frac{U[\mu]_l - g[\rho]_l}{3T_1}\right)^{3/2}, Q_{r,\max}(\lambda_2 = 1)\right\}\Bigg), \\ = \sigma_1^u, & \end{aligned} \tag{24}$$

where

$$Q_{l,\max}(\lambda_1 = 1) = \max_k\left(\frac{k(U[\mu]_l - g[\rho]_l) - T_1 k^3}{\mu_l + \mu_1 \tanh(kL)}\right) = \left(\frac{k_1^*(U[\mu]_l - g[\rho]_l) - T_1 (k_1^*)^3}{\mu_l + \mu_1 \tanh(k_1^* L)}\right), \tag{25}$$

and k_1^* is the value of k that solves the following equation.

$$\frac{k(U[\mu]_l - g[\rho]_l) - T_1 k^3}{\mu_l + \mu_1 \tanh(kL)} = \frac{(U[\mu]_l - g[\rho]_l - 3T_1 k^2)\cosh^2(kL)}{\mu_1 L}. \tag{26}$$

Similarly, formulae analogous to (25) and (26) can be written down for $Q_{r,\max}(\lambda_2 = 1)$ and corresponding value of k_0^* respectively. The notation k_0^* is a departure from the notation k_2^* used in a similar place in Daripa [4]. One has to take recourse to numerical computation to first find k_1^*, k_0^* from (26) etc., and then find the upper bound σ_1^u using the formulae (24). An approximation σ_1^a of the bound σ_1^u that does not require numerical computation is given by

$$\begin{aligned} \sigma_1(k) \le \min\Bigg(&\max\left\{\frac{2T_1}{\mu_l + \mu_1 c_1}\left(\frac{U[\mu]_l - g[\rho]_l}{3T_1}\right)^{3/2}, \frac{2T_0}{\mu_r}\left(\frac{U[\mu]_r - g[\rho]_r}{3T_0}\right)^{3/2}\right\}, \\ &\max\left\{\frac{2T_1}{\mu_l}\left(\frac{U[\mu]_l - g[\rho]_r}{3T_1}\right)^{3/2}, \frac{2T_0}{\mu_r + \mu_1 c_0}\left(\frac{U[\mu]_r - g[\rho]_r}{3T_0}\right)^{3/2}\right\}\Bigg) \\ = \sigma_1^a \sim \sigma_1^u. & \end{aligned} \tag{27}$$

where $0 < c_1 \le \tanh(k_{c1} L)$ and $0 < c_0 \le \tanh(k_{c0} L)$. The constants k_{c1} and k_{c0} have been defined in (23).

3.4 Stability enhancement

Presence of gravity certainly alters the landscape of stability enhancement strategies due to the presence of Rayleigh-Taylor instability. For two-layer flows, a reduction in forward jump (i.e., jump in the direction of upstream flow) in viscosity $(\mu_r - \mu_l)$ or/and an increase in forward jump in density $(\rho_r - \rho_l)$ (see equation (2)) at an unstable interface has a stabilizing effect whereas a reduction in the value of interfacial tension has a destabilizing effect. Therefore, stabilizing an unstable interface in an otherwise two-layer flow (fluid with viscosity μ_l pushing fluid with viscosity μ_r) by introducing a third fluid having viscosity

μ_1 with $\mu_l < \mu_1 < \mu_r$ (notations have been discussed above) requires that interfacial tensions and density of the middle-layer fluid must have reasonable values not to offset any gain in stabilization due to reduction in viscosity jump at the leading interface in this three-layer set-up. It is of interest to be able to quantify this in terms of fluid viscosities, fluid densities, and interfacial tensions for the three-layer flows. We will do this below in this section after discussing the roles of short and long waves in this stabilization process.

Since interfacial tension primarily affects short waves and not long waves, it is possible that middle-layer fluid with (i) $\mu_l < \mu_1 < \mu_r$ and $\rho_l \geq \rho_1 > \rho_r$ or (ii) $\mu_l \leq \mu_1 < \mu_r$ and $\rho_l > \rho_1 > \rho_r$ in the three-layer flow suppresses instability of long waves regardless of interfacial tension values at the two interfaces. We need to mathematically investigate this issue in this three-layer case. If this is indeed the case (as we will see below), then it will allow us to obtain estimates for the constants c_0 and c_1 that appear in the formula (27).

3.4.1 Long and Short waves

From approximate modal upper bound $\sigma_{1,l}^m(k;\lambda_1,\lambda_2)$ for long waves ($kL << 1$), inequality (22) is approximated as

$$\sigma_{1,l}(k) < \sigma_{1,l}^m(k;\lambda_1,\lambda_2) \approx \max\left\{\frac{k(U(\mu_1-\mu_l)-g(\rho_1-\rho_l))}{\mu_l+\lambda_1 k\,L\,\mu_1}, \quad \frac{k(U(\mu_r-\mu_1)-g(\rho_r-\rho_1))}{\mu_r+\lambda_2 k\,L\,\mu_1}\right\}. \tag{28}$$

Using this, one can show that all long waves are stabilized on at least on one of the two interfaces regardless of the values of the interfacial tensions, i.e., they will be less unstable than on a Taylor-unstable interface separating two extreme-layer fluids having $\mu_r > \mu_l$. In fact, following the procedure outlined in Daripa [4], it can be seen that inequalities

$$(U\mu_1 - g\rho_1) < (U\mu_l - g\rho_l) + \frac{U(\mu_r-\mu_l)-g(\rho_r-\rho_l)}{\mu_r+\mu_l}\mu_r(1+L). \tag{29}$$

and

$$(U\mu_r - g\rho_r) - \frac{U(\mu_r-\mu_l)-g(\rho_r-\rho_l)}{\mu_r+\mu_l}\mu_r(1+L) < (U\mu_1 - g\rho_1). \tag{30}$$

are necessary and sufficient for stabilization of long waves on **both** the interfaces assuming as always $\mu_r > \mu_l$. The subscript s below is used on σ for the short wave regime, $kL \geq 1$.

$$\sigma_{1,s}(k) \leq \sigma_{1,s}^m(k;\lambda_1,\lambda_2) = \max_{\lambda_1+\lambda_2\leq 1}\left\{\frac{k(U[\mu]_l - g[\rho]_l) - k^3 T_1}{\mu_l+\lambda_1 c_1\mu_1}, \quad \frac{k(U[\mu]_r - g[\rho]_r) - k^3\,T_0}{\mu_r+\lambda_2 c_0\mu_1}\right\}, \tag{31}$$

where $\lambda_i \geq 0$ and c_1, c_0 are suitable constants mentioned above after equation (27).

3.4.2 Necessary and Sufficient conditions for stability enhancement

Condition of stabilization due to an introduction of an intermediate layer is $\sigma_1^u < \sigma_t^u$. An approximation to this is $\sigma_1^a < \sigma_t^u$ where σ_1^a is given by (27) and σ_t^u by (2). Letting $c_1 = c_0 = c$ in (27) and then manipulating this approximate inequality give following sufficient conditions for total stabilization (i.e. reduction in maximum growth rates of disturbances on both the interfaces).

$$(U\mu_1 - g\rho_1) < (U\mu_l - g\rho_l) + \left(\frac{T_1}{T}\right)^{1/3}\left(\frac{\mu_{1l}}{\mu_l+\mu_r}\right)^{2/3}(U(\mu_r-\mu_l)-g(\rho_r-\rho_l)), \tag{32}$$

and

$$(U\mu_r - g\rho_r) < \left(\frac{T_0}{T}\right)^{1/3}\left(\frac{\mu_{r1}}{\mu_l + \mu_r}\right)^{2/3}(U(\mu_r - \mu_l) - g(\rho_r - \rho_l)) + (U\mu_1 - g\rho_1), \tag{33}$$

where

$$\mu_{1l} = (\mu_l + \lambda_1\mu_1\, c), \quad \text{and} \quad \mu_{r1} = (\mu_r + \lambda_2\mu_1\, c). \tag{34}$$

It is easy to see that the following necessary condition (parameterized by two parameters λ_1 and λ_2) for total stabilization which is also a sufficient condition for partial stabilization (i.e., stabilization of at least one of the two interfaces) follows from these inequalities.

$$\left(\frac{T_0}{T}\right)^{1/3} + \left(\frac{\mu_l + \lambda_1\mu_1 c}{\mu_r + \lambda_2\mu_1 c}\right)^{2/3}\left(\frac{T_1}{T}\right)^{1/3} > \left(\frac{\mu_r + \mu_l}{\mu_r + \lambda_2\mu_1 c}\right)^{2/3}. \tag{35}$$

Since this condition is parameterised by λ_1 and λ_2 which can take values in a range mentioned in the lemma (see section 3.1), it is clear that there is a wide selection possibilities of interfacial tensions and middle layer fluid that will guarantee stabilization but for best stabilization as discussed before choice of (λ_1, λ_2) should be either (1,0) or (1,0).

The following specific points about above sufficient conditions for total and partial stabilizations are worth highlighting here.

- The sufficient conditions for total and partial stabilizations depend always (i.e., for all admissible values of λ_1 and λ_2) on all three interfacial tensions.
- The sufficient (also necessary) conditions (32) and (33) for total stabilization depend on gravity and hence on ST-instability. In other words, densities of fluids affect the criteria for stabilizations of both the interfaces which, in general, is expected.
- Interestingly, the sufficient condition (35) for partial stabilization does not depend on the density of any of the fluids. Therefore, effect of RT-instability can be ignored while making choices of viscosities and interfacial tensions based on (35) which will guarantee stabilization of one of the interfaces. This result is unusual and non-intuitive.
- The condition (35) does not depend on the viscosity of the middle layer when $(\lambda_1, \lambda_2) = (0, 0)$. When all three interfacial tensions are same, partial stabilization is always ensured since the resulting inequality from (35) holds regardless of the values of viscosities, densities, and equal interfacial tensions.

4 Constant viscosity fluid layers: Four-layer case

The set-up shown in Fig. 2 is self-explanatory and is an extension of the three-layer case. It has now three interfaces located at $x = 0$, $x = -L$, and $x = -2L$ in the frame moving with speed U. The gravity acts in the direction of U and each layer has constant density which can be different in different layers. The constant densities of fluids are denoted similar to the viscosities but with conventional notation ρ.

We first treat the case where the density jump at each of the interfaces is either positive or negative in the direction of flow so long as each of the interfaces is overall individually unstable. The field equation (5) holds away from all three interfaces and hence the far-field behavior (6), with L there

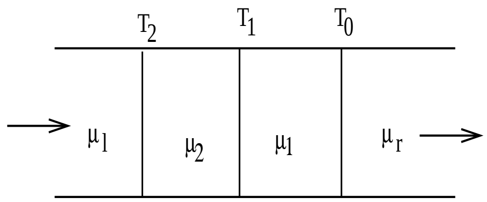

Figure 2: Four-layer fluid flow in a Hele-Shaw cell. Interfacial tensions at three interfaces are shown as T_0, T_1, and T_2. The constant viscosities are increasing in the direction of flow: $\mu_l < \mu_2 < \mu_1 < \mu_r$.

replaced by $2L$, holds in the exterior layers of fluid. The dynamic and kinematic interfacial conditions are similar to the ones given in section 4 of Daripa [4] except that each of the interfacial viscosity jumps there is modified by adding $-g[\rho]/U$ to it where $[\rho]$ denotes the density jump at that interface in the flow direction. Other than this, further analysis identical to the one in that paper leads to the following modal upper bound on the growth rate σ_2, subscript 2 on σ stands for number of layers which is two for the four-layer (two external and two internal layers) case.

$$\sigma_2(k) \leq \frac{E_0 f^2(0) + E_1 f^2(-L) + E_2 f^2(-2L)}{F_0 f^2(0) + F_1 f^2(-L) + F_2 f^2(-2L)}, \tag{36}$$

where E_i's and F_i's are defined by

$$\left.\begin{aligned} E_0 &= k^2\left(U(\mu_r - \mu_1) - g(\rho_r - \rho_1)\right) - k^4 T_0, \\ E_1 &= k^2\left(U(\mu_1 - \mu_2) - g(\rho_1 - \rho_2)\right) - k^4 T_1, \\ E_2 &= k^2\left(U(\mu_2 - \mu_l) - g(\rho_2 - \rho_l)\right) - k^4 T_2. \end{aligned}\right\} \qquad \left.\begin{aligned} F_0 &= k\left\{\mu_1 \lambda_{2,1} \tanh(kL) + \mu_r\right\}, \\ F_1 &= k\left(\mu_1 \lambda_{1,1} + \mu_2 \lambda_{2,2}\right) \tanh(kL), \\ F_2 &= k\left\{\mu_l + \mu_2 \lambda_{1,2} \tanh(kL)\right\}. \end{aligned}\right\} \tag{37}$$

According to the lemma, $\lambda_{1,1} + \lambda_{2,1} \leq 1$ and $\lambda_{1,2} + \lambda_{2,2} \leq 1$ where each of these $\lambda_{i,j} \geq 0$. To obtain an upper bound from applying the inequality (10) to (36) (see below), F_1 can not be zero. This means that in this 4-layer case, we have another constraint, namely the coefficients $\lambda_{1,1}$ and $\lambda_{2,2}$ can not be simultaneously zero or equivalently

$$\underline{\lambda_{1,1} + \lambda_{2,2} > 0.} \tag{38}$$

Following procedure given in Darpia [4] (see also section 3 of this paper), following estimate of the modal upper bound on the growth rate of all waves is obtained.

$$\begin{aligned} \sigma_2(k) &\leq \max_{\lambda_{1,j}+\lambda_{2,j}=1} \{Q_0, Q_1, Q_2\} \\ &= \sigma_2^m(k; \lambda_{1,1}, \lambda_{2,1}, \lambda_{1,2}, \lambda_{2,2}) \equiv \sigma_2^m(k; \lambda_{i,j}), \end{aligned} \tag{39}$$

where

$$\left.\begin{aligned} Q_0(k, \lambda_{2,1}) &= E_0/F_0 = k(U[\mu]_0 - g[\rho]_0 - T_0 k^2)/(\mu_r + \lambda_{2,1}\mu_1 \tanh(kL)), \\ Q_1(k, \lambda_{1,1}, \lambda_{2,2}) &= E_1/F_1 = k(U[\mu]_1 - g[\rho]_1 - T_1\, k^2)/((\mu_l \lambda_{1,1} + \mu_2 \lambda_{2,2}) \tanh(kL)), \\ Q_2(k, \lambda_{1,2}) &= E_2/F_2 = k(U[\mu]_2 - g[\rho]_2 - T_2 k^2)/(\mu_l + \lambda_{1,2}\mu_2 \tanh(kL)). \end{aligned}\right\} \tag{40}$$

and $[\mu]_0 = (\mu_r - \mu_1)$, $[\mu]_1 = (\mu_1 - \mu_2)$, $[\mu]_2 = (\mu_2 - \mu_l)$. Similarly, for the definitions of $[\rho]$. The $Q_0(k, \lambda_{2,1})$, $Q_1(k, \lambda_{1,1}, \lambda_{2,2}), Q_2(k, \lambda_{1,2})$ are effective modal growth rates of disturbances on the leading (right-most interface in the figure), internal and left-most interfaces respectively. It is worth drawing attention to the similarity in the form of the effective growth rates $Q_0(k, \lambda_{2,1})$ and $Q_2(k, \lambda_{1,2})$ of the two external interfaces and to the difference between these and the effective growth rate $Q_1(k, \lambda_{1,1}, \lambda_{2,2})$ of the internal interface. We have four families of upper bounds in (40) due to four parameters $\lambda_{1,2}, \lambda_{2,2}, \lambda_{1,1}, \lambda_{2,1}$. *Some simple upper bounds (strict inequality) will result from choosing anyone of these four λ's one and rest all zero with the exception of the case $\lambda_{1,1} = \lambda_{2,2} = 0$ due to* (38). This leaves only the following two choices: (i) $\lambda_{1,1} = 1, \lambda_{1,2} = \lambda_{2,2} = \lambda_{2,1} = 0$; and (ii) $\lambda_{2,2} = 1, \lambda_{1,2} = \lambda_{1,1} = \lambda_{2,1} = 0$. For these choices, some of the terms in the denominator of (36) are essentially neglected. For other choices (see the Lemma) such that $\lambda_{1,1} + \lambda_{2,1} < 1$ and/or $\lambda_{1,2} + \lambda_{2,2} < 1$, the modal upper bound $\sigma_2^m(k; \lambda_{ij})$ is also a strict inequality. There are many choices (e.g., $\lambda_{1,1} > 0$ or/and $\lambda_{2,1} > 0$) for which $\sigma_2^m(k; \lambda_{ij})$ is also a strict inequality. The modal upper bound $\sigma_2^m(k; \lambda_{ij})$ for $\lambda_{1,2} = \lambda_{2,2} = \lambda_{1,1} = \lambda_{2,1} = \frac{1}{2}$, which is an interesting upper bound because of the symmetry, may be approachable because the bound in this case is not a strict inequality.

4.1 Optimal estimates of modal and absolute upper bounds

Following the procedure of subsection 3.3, the formula for the best estimates of the modal and absolute upper bounds are as follows for the four layer case. The corresponding formulas for the three-layer case are (22) and (24). It will be easier to understand the formulae for upper bounds below if we just recall here the order in which the dependency of σ_2^m on the parameters appears in $\sigma_2^m(k; \lambda_{1,1}, \lambda_{2,1}, \lambda_{1,2}, \lambda_{2,2})$. For the model upper bound $\sigma_2^m(k)$, we obtain

$$\begin{aligned}
\sigma_2(k) &\leq \min\left(\sigma_2^m(k; 1, 0, 1, 0), \sigma_2^m(k; 1, 0, 0, 1), \sigma_2^m(k; 0, 1, 0, 1)\right) \\
&= \min\left(\max\left\{Q_0(k, \lambda_{2,1} = 0), Q_1(k, \lambda_{1,1} = 1, \lambda_{2,2} = 0), Q_2(k, \lambda_{1,2} = 1)\right\},\right. \\
&\qquad \max\left\{Q_0(k, \lambda_{2,1} = 0), Q_1(k, \lambda_{1,1} = 1, \lambda_{2,2} = 1), Q_2(k, \lambda_{1,2} = 0)\right\}, \\
&\qquad \left.\max\left\{Q_0(k, \lambda_{2,1} = 1), Q_1(k, \lambda_{1,1} = 0, \lambda_{2,2} = 1), Q_2(k, \lambda_{1,2} = 0)\right\}\right) \\
&= \sigma_2^m(k).
\end{aligned} \tag{41}$$

Note that $\sigma_2^m(k; 0, 1, 1, 0)$ is not included above because it corresponds to choice of $\lambda_{1,1} = \lambda_{2,2} = 0$ which does not satisfy the constraint (38). For the absolute upper bound σ_2^u, we have from the analysis of $\sigma_2^m(k)$ the following.

$$\begin{aligned}
\sigma_2(k) \leq \min &\left(\max\left\{\frac{2T_0}{\mu_r}\left(\frac{U[\mu]_0 - g[\rho]_0}{3T_0}\right)^{3/2}, Q_{1,\max}(\lambda_{1,1} = 1, \lambda_{2,2} = 0), Q_{2,\max}(\lambda_{1,2} = 1),\right\},\right. \\
&\max\left\{\frac{2T_0}{\mu_r}\left(\frac{U[\mu]_0 - g[\rho]_0}{3T_0}\right)^{3/2}, Q_{1,\max}(\lambda_{1,1} = 1, \lambda_{2,2} = 1), \frac{2T_2}{\mu_l}\left(\frac{U[\mu]_2 - g[\rho]_2}{3T_2}\right)^{3/2}\right\}, \\
&\left.\max\left\{Q_{0,\max}(\lambda_{2,1} = 1), Q_{1,\max}(\lambda_{1,1} = 0, \lambda_{2,2} = 1), \frac{2T_2}{\mu_l}\left(\frac{U[\mu]_2 - g[\rho]_2}{3T_2}\right)^{3/2}\right\}\right) \\
= \sigma_2^u, &
\end{aligned} \tag{42}$$

where, for the three specific choices of the pair $(\lambda_{1,1}, \lambda_{2,2})$ which appear in (41),

$$Q_{1,\max}(\lambda_{1,1}, \lambda_{2,2}) = \max_k \left(\frac{k(U[\mu]_1 - g[\rho]_1) - T_1 k^3}{(\mu_l \lambda_{1,1} + \mu_2 \lambda_{2,2}) \tanh(kL)}\right) \approx \frac{U[\mu]_1 - g[\rho]_1}{L(\mu_l \lambda_{1,1} + \mu_2 \lambda_{2,2})}. \tag{43}$$

and

$$Q_{2,\max}(\lambda_{1,2} = 1) = \max_k \left(\frac{k(U[\mu]_2 - g[\rho]_2) - T_2 k^3}{\mu_l + \mu_2 \tanh(kL)}\right) = \left(\frac{k_2^\dagger(U[\mu]_2 - g[\rho]_2) - T_2 (k_2^\dagger)^3}{\mu_l + \mu_2 \tanh(k_2^\dagger L)}\right), \tag{44}$$

with $k_2^\dagger$ as the solution of the following equation.

$$\frac{k(U[\mu]_2 - g[\rho]_2) - T_2 k^3}{\mu_l + \mu_2 \tanh(kL)} = \frac{(U[\mu]_2 - g[\rho]_2 - 3T_2 k^2)\cosh^2(kL)}{\mu_2\, L}. \tag{45}$$

Similarly, formulae analogous to (44) and (45) can be written down for $Q_{0,\max}(\lambda_{2,1} = 1)$ and corresponding $k_0^\dagger$ respectively.

Now, with all the details given above, the absolute upper bound σ_2^u can be evaluated from (42) only after $k_0^\dagger$ and $k_2^\dagger$ have been found numerically. Approximate formulas for $Q_{0,\max}(\lambda_{2,1} = 1)$ and $Q_{2,\max}(\lambda_{1,2} = 1)$ that do not require any numerical evaluation of $k_0^\dagger$ and $k_2^\dagger$ can be obtained using the same procedure as in subsection 3.3. Using such procedure and (43) in (42), the following approximate upper bound σ_2^a is obtained.

$$\begin{aligned}\sigma_2(k) \leq \min\Bigg(&\max\left\{\frac{2T_0}{\mu_r}\left(\frac{U[\mu]_0 - g[\rho]_0}{3T_0}\right)^{3/2}, \frac{U[\mu]_1 - g[\rho]_1}{L\mu_l}, \frac{2T_2}{\mu_l + \mu_2\, c_2^\dagger}\left(\frac{U[\mu]_2 - g[\rho]_2}{3T_2}\right)^{3/2}\right\}, \\ &\max\left\{\frac{2T_0}{\mu_r}\left(\frac{U[\mu]_0 - g[\rho]_0}{3T_0}\right)^{3/2}, \frac{U[\mu]_1 - g[\rho]_1}{L(\mu_l + \mu_2)}, \frac{2T_2}{\mu_l}\left(\frac{U[\mu]_2 - g[\rho]_2}{3T_2}\right)^{3/2}\right\}, \\ &\max\left\{\frac{2T_0}{\mu_r + \mu_1\, c_0^\dagger}\left(\frac{U[\mu]_0 - g[\rho]_0}{3T_0}\right)^{3/2}, \frac{U[\mu]_1 - g[\rho]_1}{L\mu_2}, \frac{2T_2}{\mu_l}\left(\frac{U[\mu]_2 - g[\rho]_2}{3T_2}\right)^{3/2}\right\}\Bigg) \\ = \sigma_2^a \sim \sigma_2^u.\end{aligned} \tag{46}$$

For selection of values for $c_0^\dagger$ and $c_2^\dagger$, the procedure discussed in subsection 3.3 for selection of values for c_0 and c_1 can be used. Specifically, as justified there, $c_0^\dagger \leq \tanh(k_0^\dagger L)$ and $c_2^\dagger \leq \tanh(k_2^\dagger L)$ and these can be chosen approximately less than or equal to $\tanh(1) = 0.76$, i.e., $c_0^\dagger = c_2^\dagger = c^\dagger$ (see subsection 3.4.1) with $c^\dagger \leq \tanh(1) = 0.7616$, preferably with equal sign for obvious reasons.

4.2 Long and short waves

For long waves $kL << 1$, the modal upper bound (39) can be approximated as

$$\begin{aligned}\sigma_{2,l}(k) &\leq \max\left\{\frac{k(U[\mu]_2 - g[\rho]_2)}{\mu_l + \lambda_{1,2}\mu_2 kL},\ \frac{U[\mu]_1 - g[\rho]_1}{L(\lambda_{2,2}\mu_2 + \lambda_{1,1}\mu_1)},\ \frac{k(U[\mu]_0 - g[\rho]_0)}{\mu_r + \lambda_{2,1}\mu_1 kL}\right\}, \\ &= \sigma_{2,l}^m(k;\lambda_{i,j}).\end{aligned} \tag{47}$$

where $[\mu]_2 = \mu_2 - \mu_l, [\mu]_1 = \mu_1 - \mu_2, [\mu]_0 = \mu_r - \mu_1$ and similarly for $[\rho]_i, i = 0, 1, 2$. Of the three terms within curly bracket above, the first and the last one correspond to the effective growth rates of long waves on the two external interfaces and the middle one corresponds to the internal interface. The second term in the above expression does not depend on k. Unless $U[\mu]_1 - g[\rho]_1 < 0$ in which case the internal interface is individually stable (i.e. stable in the absence of other interfaces), the modal upper bound (47) is not arbitrary small for long waves, i.e., when k tends to zero. Compare this with modal upper bounds $\sigma_t(k)$ (see (1)) for the two-layer case and $\sigma_{1,l}^m(k)$ (see (28)) for the three-layer case. *This shows that growth rate of long waves on the internal interface may not be less than that based on $\sigma_t(k)$ (see (1)).*

Long waves on external interfaces will be stabilized if the effective growth rates of long waves on these interfaces (i.e. first and last terms in (47)) are less than $\sigma^t(k)$ which gives two inequalities. Analyzing these two inequalities exactly the same way as in subsection 3.4.1 leads to $2\mu_r L > (\mu_l - \mu_r)$ which always holds (since $\mu_r > \mu_l$) provided the initial densities in the two internal layers are such that the internal interface is individually stable. Therefore, all long waves at least on one of the two external interfaces are stabilized in this four layer set-up provided the internal interface is individually stable. The formulas for modal and absolute upper bounds for short waves $kL \geq 1$ are similar to the ones given in section 4.1 of Daripa [4] except that each interfacial viscosity jump $[\mu]$ in those formulas must be replaced by $[\mu] - (g/U)[\rho]$ where $[\rho]$ stands for corresponding interfacial density jump. For the purposes later, an absolute upper bound (i.e., independent of k but dependent on the parameters $\lambda_{i,j}$), denoted by $\sigma^u_{2,s}(\lambda_{i,j})$ and defined by $\sigma^u_{2,s}(\lambda_{i,j}) = \max_k \{\sigma^m_{2,s}(k; \lambda_{i,j})\}$ for waves in this short wave regime is given below.

$$\begin{aligned}\sigma_{2,s}(k) \leq \max\left\{ \frac{2T_0}{\mu_{r1}} \left(\frac{U[\mu]_0 - g[\rho]_0}{3T_0}\right)^{3/2}, \; \frac{2T_1}{\mu_{12}} \left(\frac{U[\mu]_1 - g[\rho]_1}{3T_1}\right)^{3/2}, \; \frac{2T_2}{\mu_{2l}} \left(\frac{U[\mu]_2 - g[\rho]_2}{3T_2}\right)^{3/2} \right\} \\ = \sigma^u_{2,s}(\lambda_{i,j}),\end{aligned} \tag{48}$$

where

$$\mu_{r1} = (\mu_r + \lambda_{2,1}\mu_1\, c_0^\dagger), \quad \mu_{12} = (\lambda_{1,1}\mu_1 + \lambda_{2,2}\mu_2)c, \quad \mu_{2l} = (\mu_l + \lambda_{1,2}\mu_2\, c_2^\dagger). \tag{49}$$

and $[\;]_n, n = 0,1,2$ stands for jumps at the three interfaces and $\lambda_{i,j}$ can take values within the constraint of the Lemma.

4.3 Stability enhancement

Total stabilization for such 4-layer flows over the two-layer case requires that the upper bound on growth rate given by (48) be less than σ^u_t (see (2)). This leads to three conditions, similar to (32) and (33) obtained earlier in three-layer case, each corresponding to each interface.

$$\left.\begin{aligned}
(U\mu_2 - g\rho_2) < (U\mu_l - g\rho_l) + \left(\tfrac{T_2}{T}\right)^{1/3} \left(\tfrac{\mu_{2l}}{\mu_l+\mu_r}\right)^{2/3} (U(\mu_r - \mu_l) - g(\rho_r - \rho_l)), \\
(U\mu_1 - g\rho_1) < (U\mu_2 - g\rho_2) + \left(\tfrac{T_1}{T}\right)^{1/3} \left(\tfrac{\mu_{12}}{\mu_l+\mu_r}\right)^{2/3} (U(\mu_r - \mu_l) - g(\rho_r - \rho_l)), \\
(U\mu_r - g\rho_r) < (U\mu_1 - g\rho_1) + \left(\tfrac{T_0}{T}\right)^{1/3} \left(\tfrac{\mu_{r1}}{\mu_l+\mu_r}\right)^{2/3} (U(\mu_r - \mu_l) - g(\rho_r - \rho_l)),
\end{aligned}\right\} \tag{50}$$

where μ_{2l} and μ_{r1} have been defined in (49). These are sufficient conditions for total stabilization. It is easy to see that the following criterion (similar criterion for three layer case can be obtained in section 3.4.2) follows from above three conditions if $\sigma^u_t > 0$.

$$1 < \sum_{i=0}^{i=2} \left(\frac{T_i}{T}\right)^{1/3} \left(\frac{\mu_{i,i+1}}{\mu_l + \mu_r}\right)^{2/3}, \tag{51}$$

where $\mu_{0,1} = \mu_{r1}$ and $\mu_{2,3} = \mu_{2l}$ as defined above in (49). Therefore this is a necessary condition for total stabilization and not a sufficient one as the three conditions (50) do not follow from (51). However, it is easy to see from properties of inequalities that at least one of these the three conditions must hold if inequality (51) holds when $\sigma^u_t > 0$. Therefore, this inequality (51) is a sufficient condition for partial stabilization when $\sigma^u_t > 0$.

When the internal interface is individually stable, $(U\mu_1 - g\rho_1) < (U\mu_2 - g\rho_2)$. It follows from this, the first, and the third inequalities of (50) that if $\sigma^u_t > 0$, then

$$1 < \left(\frac{T_0}{T}\right)^{1/3} \left(\frac{\mu_{0,1}}{\mu_l + \mu_r}\right)^{2/3} + \left(\frac{T_1}{T}\right)^{1/3} \left(\frac{\mu_{1,2}}{\mu_l + \mu_r}\right)^{2/3} \tag{52}$$

Note that this is a less restrictive condition than (50) and is a necessary condition for total stabilization. However, this is now only a sufficient condition for stabilization of at least one of the two external interfaces while the the middle interface by the very second inequality (50) is already stable.

5 Constant viscosity multi-fluid layers: General multi-layer case

This is an extension of our studies in previous two sections to multi-layer case involving N intermediate regions of equal length L in the interval $(-NL, 0)$ where N is an arbitrary number. A fluid of constant viscosity μ_l occupies the left-most region $x < -NL$ and another fluid of constant viscosity μ_r occupies the right-most infinite region $x > 0$. The region $(-pL, -pL + L)$, $1 \leq p \leq N$ has a fluid of constant viscosity μ_p such that $\mu_l = \mu_{N+1} < \mu_N < \mu_{N-1} < ... < \mu_p < \mu_{p+1} < ... < \mu_1 < \mu_0 = \mu_r$. Similar convention is used for labeling density of fluids in various layers so that labeling index for viscosity and density for a specific layer is the same. There are $(N+1)$ interfaces located at $x_i = -iL$, $i = 0, 1, 2...N$ and labeled as i^{th} interface. Interfacial tension on the i^{th} interface at $x = x_i$ is denoted by T_i for $i = 0, 1, .., N$. Similarly, $[\mu]_i = \mu_i - \mu_{i+1}$ denotes the viscosity jump at the i^{th} interface for $i = 0, 1, ..., N$. The flow is in the direction of increasing viscosity.

Procedure of the previous sections and, in particular, that of section 5 of Daripa [4] leade to the following estimate of the modal upper bound on the growth rates of all waves.

$$\begin{aligned}
\sigma_N(k) &\leq \max_{\lambda_{1,i}+\lambda_{2,i}=1} \left\{ \frac{E_0}{F_0}, \frac{E_1}{F_1}, \ldots, \frac{E_i}{F_i}, \ldots, \frac{E_{N-1}}{F_{N-1}}, \frac{E_N}{F_N} \right\} \\
&\leq \max_{\lambda_{1,i}+\lambda_{2,i}=1} \{Q_0,\ Q_1, \ldots, Q_i, \ldots, Q_{N-1}, Q_N\} \\
&= \sigma_N^m(k; \lambda_{i,j}),
\end{aligned} \tag{53}$$

where

$$\begin{aligned}
Q_0 &= \frac{E_0}{F_0} = \frac{k(U[\mu]_0 - g[\rho]_0) - k^3\, T_0}{(\mu_r + \lambda_{2,1}\mu_1 \tanh(kL))}, \\
Q_i &= \frac{E_i}{F_i} = \frac{k(U[\mu]_i - g[\rho]_i) - k^3\, T_i}{(\lambda_{1,i}\mu_i + \lambda_{2,i+1}\mu_{i+1}) \tanh(kL)}, \qquad i = 1, \ldots, (N-1) \\
Q_N &= \frac{E_N}{F_N} = \frac{k(U[\mu]_N - g[\rho]_N) - k^3\, T_N}{(\mu_l + \lambda_{1,N}\mu_N \tanh(kL))}.
\end{aligned} \tag{54}$$

The absolute upper bound arising from (53) will depend on parameters $\underline{\lambda_{1,j}, \text{ and } \lambda_{2,j},\ j = 1, \ldots, N}$. Following the procedure outlined in section 4.1, one can judiciously choose the parameters $\lambda_{i,j}$ satisfying $\underline{\lambda_{1,i} + \lambda_{2,i+1} > 0}$ (so that the denominators F_is of Q_is are not zero) at all interfaces and $\underline{\lambda_{1,i} + \lambda_{2,i} = 1}$, $i = 1, \ldots\ldots N$ for the best modal upper bound $\sigma_N^m(k)$ analogous to (41), for the best absolute upper bound σ_N^u analogous to (42), and for the best approximate absolute upper bound σ_N^a analogous to (46).

5.1 Long and short waves

For long waves (i.e. $kL << 1$), similar procedure as before gives the following modal upper bound $\sigma_{N,l}^m(k; \lambda_{i,j})$.

$$\sigma_{N,l}(k) \leq \sigma_{N,l}^m(k; \lambda_{i,j}) = \max \left\{ Q_0^l, \ldots, Q_p^l, \ldots, Q_N^l \right\} \tag{55}$$

where

$$Q_N^l = \frac{k(U(\mu_N - \mu_l) - g(\rho_N - \rho_l))}{\mu_l + \mu_N \lambda_{1,N} kL}, \quad Q_0^l = \frac{k(U(\mu_r - \mu_1) - g(\rho_r - \rho_1))}{\mu_r + \mu_1 \lambda_{2,1} kL},$$
$$Q_p^l = \frac{U(\mu_p - \mu_{p+1}) - g(\rho_p - \rho_{p+1})}{(\mu_p \lambda_{1,p} + \mu_{p+1}\lambda_{2,p+1})L}, \quad p = 1, \ldots, (N-1) \tag{56}$$

Q_0^l and Q_N^l above are effective growth rates of long waves on the two external interfaces and Q_p^l for $p = 1, \ldots, N-1$ are the effective growth rates of the $(N-1)$ internal interfaces. These formulas for stability of long waves on these internal and external interfaces have similar interpretation as in the four layer case when $N = 2$ which has been discussed in section 4.2. For example, the modal upper bound is not arbitrarily small for long waves on internal interfaces and hence such long waves may not be stabilized on these internal interfaces. However, maximum growth rates on these interfaces can be made less than σ_t^u with proper choice of parameters which has been addressed in the next subsection. For exactly the same reasons as in sections 4.2, all long waves on at least one of the two external interfaces are stabilized provided the internal interfaces are individually stable on their own.

For shortwaves with $kL \geq 1$, similarly one obtains following upper bound $\sigma_{N,s}^u(\lambda_{i,j})$ on the growth rate.

$$\sigma_{N,s}(k) \leq \sigma_{N,s}^u(\lambda_{i,j}) = \max\left\{Q_0^s, \ldots, Q_p^s, \ldots, Q_N^s\right\}, \tag{57}$$

where

$$Q_0^s = \frac{2T_0}{\mu_{r1}}\left(\frac{U(\mu_r - \mu_1) - g(\rho_r - \rho_1)}{3T_0}\right)^{3/2},$$
$$Q_N^s = \frac{2T_N}{\mu_{Nl}}\left(\frac{U(\mu_N - \mu_l) - g(\rho_N - \rho_l)}{3T_N}\right)^{3/2},$$
$$Q_p^s = \frac{2T_p}{\mu_{p,p+1}}\left(\frac{U(\mu_p - \mu_{p+1}) - g(\rho_p - \rho_{p+1})}{3T_p}\right)^{3/2}, \quad p = 1, 2, \ldots, (N-1) \tag{58}$$

Above we have use the following notations:

$$\left.\begin{aligned} &\mu_{0,1} \equiv \mu_{r1} = \mu_r + \lambda_{2,1}\mu_1\, c, \\ &\mu_{i,i+1} = (\lambda_{1,i}\mu_i + \lambda_{2,i+1}\mu_{i+1})c, \quad i = 1, 2, \ldots, (N-1) \\ &\mu_{N,N+1} \equiv \mu_{Nl} = \mu_l + \lambda_{1,N}\mu_N\, c. \end{aligned}\right\} \tag{59}$$

where $c \approx \tanh(1)$. An absolute upper bound $\sigma_{N,s}^u$ dependent on parameters $\lambda_{i,j}$ easily follows from (57) using the same procedure as in subsection 4.2. This will result in a formula similar to (48) except that there will be $N+1$ similar terms, each one corresponding to one interface, instead of three as it appears in (48). One most important thing to note that as before this formula in fact is also an excellent approximation for the absolute upper bound over the entire spectrum, not just short waves for the same reasons mentioned in the 3-layer case.

5.2 Stability enhancement

Analogous to the 4-layer case, sufficient conditions for stabilization are the following N inequalities.

$$(U\mu_i - g\rho_i) < \left(\frac{T_i}{T}\right)^{\frac{1}{3}}\left(\frac{\mu_{i,i+1}}{\mu_l + \mu_r}\right)^{\frac{2}{3}} + (U\mu_{i+1} - g\rho_{i+1}); i = 0, 1, 2, \ldots.., N \tag{60}$$

If $\sigma_t^u > 0$, then the following necessary condition for total stabilization of $(N+2)-$layer flows follows from the above $N+1$ conditions.

$$1 < \sum_{i=0}^{i=N} \left(\frac{T_i}{T}\right)^{1/3} \left(\frac{\mu_{i,i+1}}{\mu_l + \mu_r}\right)^{2/3} \tag{61}$$

Notice that it reduces to (51) in the 4-layer case as it should. Following the arguments after (51), it is easy to derive conclusions similar to the ones given there in the 4-layer case (details omitted) such as (i) inequality (61) is also a sufficient condition for partial stabilization; (ii) if one or more of the internal interfaces is individually stable on its own, then conditions less restrictive than (61) exist for total stabilization. For example, if j^{th} and l^{th} interfaces are individually stable on its own, then two terms corresponding to these two interfaces in the formula (61) need not be included in the sum and the resulting formulae will be the necessary condition for total stabilization.

6 Variable viscosity fluid layers

The physical set-up here is the same as discussed in section 5 except that each of the N internal fluid layers has a smooth viscous profile $\mu(x)$ with $\mu_x > 0$ so that each internal layer is also individually unstable. The case when one or more of these internal layers has constant viscosity is also included in the following treatment. The field equation in each internal layer is now defined by general equation (4). This equation simplifies to (5) in the exterior layers: $x < -NL, x > 0$. Because of this, the far-field behavior is external layers are same as previous cases. Following procedure similar as before, following interfacial boundary conditions at $x = -NL, \ldots\ x = -L$, $x = 0$ are obtained.

$$\left.\begin{array}{l} -(\mu^- f_x^- f)(0) = \mu_r\, k f^2(0) - \sigma^{-1} E_0\, f^2(0), \\ (\mu^+ f_x^+ f)(-pL) - (\mu^- f_x^- f)(-pL) = -\sigma^{-1} E_p\, f^2(-L),\ p = 1, ..., N-1 \\ (\mu^+ f_x^+ f)(-NL) = \mu_l\, k f^2(-NL) - \sigma^{-1} E_N\, f^2(-NL), \end{array}\right\} \tag{62}$$

where $E_i = k^2(U[\mu]_i - g[\rho]_i) - k^4\, T_i, \quad i = 0, 1, \ldots, N$ with $[\mu]_0 = [\mu]_r = (\mu_r - \mu^-(0))$, $[\mu]_p = (\mu^+(-pL) - \mu^-(-pL))$, $p = 1, \ldots (N-1)$ and $[\mu]_N = [\mu]_l = (\mu^+(-NL) - \mu_l)$. Similarly for $[\rho]_r$, $[\rho]_p$, $p = 1, \ldots (N-1)$ and $[\rho]_l$. Multiplying variable viscosity field equation (4) by $f(x)$ and then integrating across the N internal layers $(-NL, 0)$, we get

$$(\mu^+ f_x^+ f)(-NL) + \sum_{p=1}^{p=N-1} [(\mu^- f_x^- f)]_p - (\mu^- f_x^- f)(0) + \int_{-NL}^{0} \mu f_x^2\, dx + \\ + k^2 \int_{-NL}^{0} \mu\, f^2\, dx = \sigma^{-1} k^2 U \int_{-NL}^{0} \mu_x f^2\, dx. \tag{63}$$

Above $[\ ]_p$ denotes jump in the bracketed quantity in the direction of flow at the p^{th} internal interface. Since $\mu(x), f_x(x)$ are discontinuous at the interior interface locations $x = -(N-1)L, \ldots, -L$, the integrals needs to be split into N parts, each spanning over one internal layer. Thus we get using relations (62) in (63) and then simplifying

$$\sigma = \frac{\sum_{p=0}^{p=N} E_p f^2(-pL) + k^2\, U \int_{-NL}^{0} \mu_x\, f^2}{\mu_l\, k f^2(-NL) + \mu_r\, k f^2(0) + \int_{-NL}^{0} \mu(f_x^2 + k^2 f^2)\, dx}. \tag{64}$$

Here also, as before, it is adequate for the purpose of estimating the upper bound to analyze (64) over the wavenumber in the range given by $k^2 \leq \min(U(\mu_i - \mu_{i+1}) - g(\rho_i - \rho_{i+1})/T_i), i = 0, 1, ..., N$ for which all $E_i > 0, i = 0, \ldots, N$. In such case, it is obvious that all interfaces are individually unstable on its own. If one or more of these interfaces is individually stable, then these interfaces do not participate in the analysis for estimating upper bound.

For 3-layer case $N = 1$, it is straightforward (see previous sections) to apply the inequality (10) as we have done in previous sections to (64). This leads to the following absolute upper bound in strict inequality form similar to the result already presented in [4] except for the density jump term below.

$$\sigma_1 \leq \max\left\{ \frac{2T_0}{\mu_r}\left(\frac{U[\mu]_r - g[\rho]_r}{3T_0}\right)^{3/2}, \ \frac{2T_1}{\mu_l}\left(\frac{U[\mu]_l - g[\rho]_l}{3T_1}\right)^{3/2}, \ \frac{U}{\mu_l}\sup_x\{\mu_x\} \right\} = \sigma_1^u. \tag{65}$$

However, for flows involving more than 4 layers it is not so obvious how (64) can be reduced to a form to which the inequality (10) can be applied to obtain an estimate of the absolute upper bound similar to the above 3-layer case. However, it becomes possible if all the internal interfaces are individually stable, i.e., when density stratification across each of the internal interfaces is stable enough to offset the interfacial Saffman-Taylor instability induced by unfavorable viscosity jumps across these internal interfaces. For instance, in the four layer ($N = 2$) case, (64) becomes

$$\sigma = \frac{E_2 f^2(-2L) + E_1 f^2(-L) + E_0 f^2(0) + k^2\, U \int_{-2L}^{0} \mu_x\, f^2}{\mu_l\, k f^2(-2L) + \mu_r\, k f^2(0) + \int_{-2L}^{0} \mu (f_x^2 + k^2 f^2)\, dx}. \tag{66}$$

Since $E_1 < 0$ because the internal interface is individually stable, the term involving E_1 can be dropped which reduces (66) to a form to which the inequality (10) can be applied to obtain an estimate of the absolute upper bound resulting in

$$\begin{aligned}\sigma &< \max\left\{ \frac{2T_0}{\mu_r}\left(\frac{U[\mu]_r - g[\rho]_r}{3T_0}\right)^{3/2}, \ \frac{2T_2}{\mu_l}\left(\frac{U[\mu]_l - g[\rho]_l}{3T_2}\right)^{3/2}, \ \frac{U}{\mu_l}\sup_x\{\mu_x\,|x \neq -L, -2L, 0\} \right\} \\ &= \sigma_2^u. \end{aligned} \tag{67}$$

Thus the absolute upper bound is given by the maximum over the effective growth rates of three entities: two external unstable interfaces and two individually unstable internal layers. Similar analysis will give exactly similar formula for layered flows with $N > 2$ (this corresponds to 4-layer flows) when all $(N-1)$ internal layers are individually stable. In this case, the absolute upper bound will be given by the maximum over the the effective growth rates of two external unstable interfaces and of $(N-1)$ unstable internal layers.

7 Conclusions

In this paper, stability of multi-layer flows is analyzed in the presence of unstable density stratification and viscosity jumps at various interfaces and also in the presence of unstable viscous profiles in various internal layers. This extends our previous work (see [4]) in many respects. Most of the mathematical analysis is similar to the case with no density stratification and physical insight as well as mathematical analysis suggests that density stratification at various interfaces is equivalent to modifying the jumps in viscosity at interfaces simply by $(-[\rho]g/U)$ where ρ is the value of the jump in density across the corresponding interface. Among many new contributions in this paper, we specifically mention the following.

1. We have introduced notions of partial and total stabilizations which helps in presenting our results concisely. For the same reasons, we have classified interfaces into two groups: internal and external interfaces.

2. For three-layer Hele-Shaw flows with **constant density and constant viscosity** layers and gravity acting in the direction of basic flow, we obtain the following results when $\sigma_t^u > 0$: (i) optimal upper bound results in exact equality forms. These show that the effective maximum growth rate at an interface can be more than when the interface is considered individually but less than σ_t^u, thus resulting in enhancement of stabilization. (ii) sufficient conditions for total stabilization which depend on fluid densities and viscosities of all three fluids as well as interfacial tensions of two interfaces; (iii) a necessary condition for total stabilization which is also a sufficient condition for partial stabilization. This condition does not depend on the densities of the fluid layers and hence this condition is the same as the one in the case when gravity is absent (see Daripa [4]); (iv) all long waves on at least one of the two interfaces are always stabilized regardless of value of the density of the middle layer.

3. Extending the 3-layer **constant-viscosity** case to the multi-layer case as such is not at all straight-forward as it may seem without a careful analysis of the 4-layer case in detail. This was missing in Daripa [4] because of which some of the restrictions on the values of the parameters $\lambda_{i,j}$ were not discovered. We have fixed this problem by first discovering the role of internal interfaces different from that of external interfaces. The 3-layer case has no internal interface as opposed to the 4-layer case where there is one internal interface. Since the internal interface responds somewhat differently in comparison to external interfaces from the standpoint of stability, the four layer case needed to be analyzed first in great detail here which made generalizing the 4-layer results to multi-layer case considerably easier, compact and correct.

4. In multi-layer flows with more than 3-layer, internal interfaces are distinctly different from the two **external interfaces** for the stability of long waves. We have obtained the following results: (i) upper bounds on growth rate; (ii) maximum growth rate at each of the interfaces can be made less than σ_t^u which gives sufficient conditions for stabilization; (iii) a necessary condition for total stabilization which also serves as a sufficient condition for partial stabilization; (iv) long waves on internal interfaces are not necessarily stabilized in multi-layer flows; (v) long waves on at least one of the two external interfaces are always stabilized.

5. Extending the 3-layer **variable-viscosity** case to the multi-layer case as such is difficult. In fact, we encountered this problem in [4] for 4-layer flows and an upper bound there could not be obtained for flows with more than three layers. This problem has been resolved here due to stable density stratification across internal interfaces which allow application of mathematical tools for estimates of upper bounds for flows with arbitrary number of layers. We have obtained an absolute upper bound on the growth rate in multi-layered flows with individually unstable viscous layers and interfaces and with favorable density stratification at internal interfaces. The upper bound

result, for optimal viscous profiles, will give similar conditions for stabilization as in the constant viscosity layer cases following the same procedure which has been discussed in section 5. We omit the details here.

In closing, we mention that quantitative results presented in this paper and techniques leading to these results are of broad interest to many areas of fundamental and applied science. We have treated the displacing fluids as Newtonian. In practice, however, most of the displacing fluids used in enhanced oil recovery are in general non-Newtonian. For example, polymeric aqueous phase is non-Newtonian and so is surfactant-laden aqueous phase with or without polymer. Interestingly, results of this paper can provide some understanding of some of the observed phenomena when non-Newtonian fluids are used. Due to shear-thinning or shear-thickening property of the non-Newtonian displacing fluid, a viscous profile is automatically created behind the displacing front due to non-uniform shear in the region behind the displacing front. Stabilizing effect of such variable viscosity profiles arising from the non-Newtonian property of complex displacing fluids can be understood within the Newtonian framework as has been shown in this paper theoretically. Such viscous profiles can be locally stabilizing or destabilizing depending on whether the viscosity gradient locally is negative or positive in the direction of flow. Recent works on viscous fingering in non-Newtonian fluids ([1], [2], [14], [15], [12], [13]) also show this to be the case even in the highly non-linear regime of viscous fingering. Therefore, in the absence of understanding based on exact non-linear theory of non-Newtonian complex fluids, our results and approach presented in this paper may be useful in interpreting some of the experimental results on viscous fingering in complex fluids. Towards this end, it is worth mentioning that stability of the system in the presence of various types of viscous profiles has been recently studied in great detail within Hele-Shaw model by Daripa & Ding [6].

In vertical displacement processes where gravity plays a decisive role, density profiles of displacing fluids also become important, in addition to the viscosity profiles, for overall stability of the displacement process. In such instances, both, Saffman-Taylor and Rayleigh-Taylor, instabilities play a role. Often there are also stratified layers of oil, water and gas whose displacements by a sequence of displacing fluids of varying viscosity and density creates a scenario which is addresses in this paper. Oil recovery for such displacement processes can be improved using results of this paper. One can use the results to design most stable displacement process. Stabler the displacement process, less severe is the fingering problem in general which is desirable for enhanced oil recovery. This entire paper is about stabilization issues and thus can be very useful. Usually, reducing the maximum growth rate of the disturbances even within linear regime has one to one correspondence with improving oil recovery. For example, one can apriori assess the stability response of a multi-layer displacement process by calculating the upper bound given in inequality (53). Thus, analyzing the parameter space on which this upper bound depends and taking into consideration various choices of displacement and displacing fluids, one can design an optimal multi-layer displacement process. For the three-layer displacement process, explicit necessary and sufficient conditions are given for optimal selection of displacing fluids that provide improved oil recovery over other choices.

Stability characteristics influence the selection of finger width among other factors. In general, stabler the system wider is the finger with flatter topology at its tip. Leaving out many factors on which finger width depends, it certainly depends on the wavenumber of most unstable wave and its growth rate. Thus the finger width for this multi-layer system usually will decrease with increasingly unstable system if one were to ignore the variation in the wavenumber of most unstable wave. Stabilization of the displacement process is likely to provide wider fingers in the non-linear regime than otherwise possible. Hopefully, future research in this direction will test the validity of this conjecture.

It is perhaps worth mentioning that during immiscible displacement processes in porous media rarefaction waves behind the displacing front create time evolving viscous and density profiles behind the displacing front. Consideration of such profiles help in the design of efficient enhanced oil recovery processes (see ([21], [22], [20]). There are other problems involving multi-layered flows of complex fluids where one of the goals is to find ways to control severe instability which can otherwise cause undesirable intermixing of the layers, particularly in thin skin coextrusion (see [19] and also [16], [17] for similar problems). The stabilization techniques similar to the ones addressed here can be useful there either directly or indirectly. We must also stress that many of the results obtained in this paper and the techniques used hold promise for applications to other unstable multi-layer flows such as Rayleigh-Taylor unstable flows, coating flows, jet-flows, and to Kelvin-Helmholtz flow, just to name a few. These results are obviously of fundamental and practical importance to many applications where stability of flows plays a decisive role.

Acknowledgments: I sincerely thank the reviewers for making useful suggestions that have helped us to improve the paper. This paper was made possible by an NPRP grant # 08-777-1-141 from the Qatar National Research Fund (a member of Qatar Foundation). The statements made herein are solely the responsibility of the author.

References

[1] Amar, M. B., and Poire, E. Pushing a non-newtonian fluid in a hele-shaw cell: From fingers to needles. *Physics of Fluids 11*, 7 (1999), 1757–1767.

[2] Chevalier, C., Ben Amar, M., D., B., and Lindner, A. Inertial effects on saffman-taylor viscous fingering. *J. Fluid Mech. 552* (2006), 83–97.

[3] Darcy, H. Les fontaines publiques de la ville de Dijon. *Paris* (1856).

[4] Daripa, P. Hydrodynamic stability of multi-layer hele-shaw flows. *Journal of Statistical Mechanics 12* (2008), 28.

[5] Daripa, P. Studies on stability in three-layer hele-shaw flows. *Phys. Fluids. 20* (2008), Article No. 112101.

[6] Daripa, P., and Ding, X. A numerical study of instability control for the design of an optimal policy of enhanced oil recovery by tertiary dispalcement processes. *Transport in Porous Media* (2012), 32.

[7] Daripa, P., and Pasa, G. New bounds for stabilizing hele-shaw flows. *Appl. Math. Lett. 18*, 11 (2005), 1293–1303.

[8] Daripa, P., and Pasa, G. A simple derivation of an upper bound in the presence of a viscosity gradient in three-layer hele-shaw flows. *Journal of Statistical Mechanics* (2006), 11 (doi:10.1088/1742–5468/2006/01/P01014).

[9] Drazin, P. G., and Reid, W. H. *Hydrodynamic Stability.* Cambridge Univ. Press., 1981.

[10] Gorell, S. B., and Homsy, G. A theory of the optimal policy of oil recovery by the secondary displacement process. *SIAM J. Appl. Math. 43* (1983), 79–98.

[11] HeleShaw, H. S. On the motion of a viscous fluid between two parallel plates. *Trans R. Inst. Na. Archit. Lond. 40* (1898), 18–.

[12] Lindner, A., Bonn, D., and Meunier, J. Viscous fingering in a shear-thinning fluid. *Physics of Fluids 12*, 2 (2000), 256–261.

[13] Lindner, A., Bonn, D., and Meunier, J. Viscous fingering in complex fluids. *Journal of Physics - Condensed Matter 12*, 8A (2000), A477–A482.

[14] Lindner, A., Bonn, D., Poire, E., Amar, M. B., and Bonn, D. Viscous fingering in non-newtonian fluids. *J. Fluid Mech. 496* (2002), 237–256.

[15] Lindner, A., Coussot, P., and Bonn, D. Viscous fingering in a yield stress fluid. *Phys. Rev. Lett. 85*, 2 (2000), 314–317.

[16] Matsunaga, K., Funatsu, K., and Kajiwar, T. Numerical simulation of multi-layer flow for polymer melts - a study of the effect of viscoelasticity on interface shape of polymers within dies. *Polymer Engineering and Science 38*, 7 (2004), 1099 – 1111.

[17] Mogavero, J., and Advani, S. Experimental investigation of flow through multi-layered preforms. *Polymer Composites 18*, 5 (2004), 649–655.

[18] Saffman, P., and Taylor, G. The penetration of a fluid into a porous medium or Hele-Shaw cell containing a more viscous liquid. *Proceedings of the Royal Society of London, Series A 245* (1958), 312–329.

[19] Schrenk, W., Bradle, N., Jr., T. A., and Maack, H. Interfacial flow instability in multilayer coextrusion. *Polymer Engineering and Science 18*, 8 (2004), 620–623.

[20] Shah, D., and Schecter, R., Eds. *Improved Oil Recovery by Surfactants and Polymer Flooding.* Academic Press, New York, NY, 1977.

[21] Slobod, R., and Lestz, J. Use of a graded viscosity zone to reduce fingering in miscible phase displacements. *Producers Monthly 24* (1960), 12–19.

[22] Uzoigwe, A., Scanlon, F., and Jewett, R. Improvement in polymer flooding: The programmed slug and the polymer-conserving agent. *J. Petrol. Tech. 26* (1974), 33–41.